Published in final edited form as:

Arterioscler Thromb Vasc Biol. 2021 September ; 41(9): 2399–2416. doi:10.1161/ATVBAHA.120.315911.

A smooth muscle cell-enriched lncRNA regulates cell plasticity and atherosclerosis by interacting with serum response factor

Huaner Ni, MD[#1,2], **Stefan Haemmig, PhD**[#1], **Yihuan Deng, PhD**[#1], **Jingshu Chen, PhD**[#1], **Viorel Simion, PhD**[1], **Dafeng Yang**[1], **Galina Sukhova, PhD**[1], **Eugenia Shvartz, BS**[1], **AKM Khyrul Wara, PhD**[1], **Henry S Cheng, PhD**[1], **Daniel Pérez-Cremades, PhD**[1], **Carmel Assa, BS**[1], **Grasiele Sausen, PhD**[1], **Rulin Zhuang, MD**[1], **Qiuyan Dai, MD, PhD**[2], **Mark W. Feinberg, MD**[1,*]

[1]Department of Medicine, Cardiovascular Division, Brigham and Women's Hospital, Harvard Medical School, Boston, MA 02115, USA;

[2]Department of Cardiology, Shanghai General Hospital, Shanghai Jiao Tong University School of Medicine, Shanghai, 200080, China.

[#] These authors contributed equally to this work.

Abstract

OBJECTIVE: Vascular smooth muscle cell (VSMC) plasticity plays a critical role in the development of atherosclerosis. Long noncoding RNAs (lncRNAs) are emerging as important regulators in the vessel wall and impact cellular function through diverse interactors. However, the role of lncRNAs in regulating VSMCs plasticity and atherosclerosis remains unclear.

APPROACH AND RESULTS: We identified a VSMC-enriched lncRNA cardiac mesoderm enhancer-associated noncoding RNA (CARMN) that is dynamically regulated with progression of atherosclerosis. In both mouse and human atherosclerotic plaques, CARMN colocalized with VSMCs and was expressed in the nucleus. Knockdown of CARMN using antisense oligonucleotides (ASO) in $Ldlr^{-/-}$ mice significantly reduced atherosclerotic lesion formation by 38% and suppressed VSMCs proliferation by 45% without affecting apoptosis. *In vitro* CARMN gain- and loss-of-function studies verified effects on VSMC proliferation, migration, and differentiation. TGF-β1 induced CARMN expression in a Smad2/3-dependent manner. CARMN regulated VSMC plasticity independent of the miR143/145 cluster, which is located in close proximity to the CARMN locus. Mechanistically, lncRNA pulldown in combination with mass spectrometry analysis showed that the nuclear-localized CARMN interacted with serum response factor (SRF) through a specific 600–1197 nucleotide domain. CARMN enhanced SRF occupancy

[*]Corresponding author: Mark W. Feinberg, Department of Medicine, Cardiovascular Division, Brigham and Women's Hospital, Harvard Medical School, Boston, MA 02115, USA. Fax: 617-525-4380; Tel: 617-525-4381. mfeinberg@bwh.harvard.edu.

Disclosures
None.

Supplemental Materials
Expanded Materials & Methods
Online Figures I – XVII
Online Tables I-V

on the promoter regions of its downstream VSMC targets. Finally, knockdown of SRF abolished the regulatory role of CARMN in VSMC plasticity.

CONCLUSIONS: The lncRNA CARMN is a critical regulator of VSMC plasticity and atherosclerosis. These findings highlight the role of a lncRNA in SRF-dependent signaling and provide implications for a range of chronic vascular occlusive disease states.

Keywords

lncRNA; CARMN; VSMCs; SRF; atherosclerosis

Introduction

Vascular smooth muscle cells (VSMCs) are a major cell type in atherosclerotic intima and play a crucial role in all stages of the atherosclerotic plaque development.[1, 2] In contrast to macrophages, VSMCs retain capacity for plasticity.[3] VSMCs phenotypic switching is a fundamental mechanism of atherosclerosis development. Classically, VSMC phenotypic switching is defined as a reversible process in which VSMCs shift from a contractile phenotype to synthetic phenotype, leading to enhanced cell proliferation, migration, and dedifferentiation.[3, 4] However, significant gaps remain in the molecular underpinnings that regulate VSMC plasticity in atherosclerotic plaques.

Several transcription and epigenetic factors have been implicated in VSMCs phenotypic switching.[5] The myocardin and serum response factor (SRF) complex increases expression of VSMC differentiation markers by binding the CArG box of target promoters.[6, 7] In contrast, Krüppel-like factor4 (KLF4), a pluripotency transcription factor, inhibits the expression of VSMC differentiation markers through its binding to a G/C repressor element.[8] VSMC phenotype is further regulated by microRNAs (miRNAs).[9] For example, the VSMC-enriched miRNA143/145 cluster, promotes cell proliferation and differentiation by directly inhibiting KLF4.[10] Expression of miRNA 143/145 is positively regulated by SRF.[11] Additionally, transforming growth factor-beta (TGF-β) plays a complex regulatory role in VSMC function and phenotypic modulation.[12, 13] TGFβ induces VSMC differentiation and promotes expression of mature VSMC genes (including ACTA2, SM22α, CNN1, and MYH11) both via the Smad2/3 signaling pathway and enhanced SRF expression.[14] However, TGF-β has also been shown to promote VSMC synthesis and secretion of collagen and proteoglycans, characteristic of a shift towards a synthetic phenotype. These seemingly antithetical effects of the TGF-β-SRF signaling pathway suggest that other factors may be involved in this regulatory axis of VSMC phenotypic switching.

Long noncoding RNAs (lncRNAs) are defined as a heterogeneous class of transcripts measuring more than 200 nucleotides in length without protein-coding potential.[15] Emerging evidence has shown that lncRNAs exert a broad range of biological functions and play a vital role in both physiologic and pathologic processes.[16, 17] LncRNAs often exhibit cell- and tissue-type-specific expression patterns, exerting crucial function in normal development and disease.[18, 19] For example, macrophage-specific lncRNA PELATON regulates phagocytosis and plaque progression in atherosclerosis.[20] VSMC-enriched

lncRNA SMILR promotes cell proliferation via direct regulation of mitotic progression.[21] However, there are few reports of lncRNAs regulating VSMC plasticity in atherosclerosis.

Here, we identified and characterized the VSMC-enriched lncRNA *CARMN* (cardiac mesoderm enhancer-associated non-coding RNA) as a critical regulator of VSMC plasticity and atherosclerosis by direct interaction with the VSMC transcription factor SRF, a key mediator of VSMC proliferation and differentiation. These findings may provide insights into the pathophysiology of a broad range of diseases characterized by vascular proliferation and remodeling.

Methods

The data that support the findings of this study are available from the corresponding author on reasonable request. All methods are described in detail in the online-only Data Supplement.

Animal experiments

Eight-week-old *Ldlr*$^{-/-}$ male mice were purchased from the Jackson Laboratory, and randomly divided into control and *CARMN* knockdown group (n=15 per group). All mice were continuously fed a high cholesterol diet (HCD, Research Diets Inc., D12108C) for 12 weeks. Control group and *CARMN* knockdown mice were intravenously injected with either a non-specific control or *CARMN* gapmeRs (10 mg/kg per mouse) twice per week. C57BL/6J mice were purchased from Charles River. All animal experiments were approved by the Institutional Animal Care and Use Committee at Brigham and Women's Hospital and Harvard Medical School, Boston, MA and conducted in accordance with the National Institutes of Health Guide for the Care and Use of Laboratory Animals. Male mice were used in this study to recapitulate the hypercholesterolemic conditions and accelerated atherosclerosis achieved as described previously with gapmeR delivery.[16, 19]

Immunohistology and characterization of atherosclerotic lesions

For the mouse atherosclerosis study, we adhered to the guidelines for experimental atherosclerosis as described in the American Heart Association Statement.[22] To characterize atherosclerotic lesions, we embedded the aortic root, and aortic arch in optimal cutting temperature (OCT) compound (Cat#23730571, Fisher Scientific, USA) after harvesting the hearts and aortas. We prepared 7-μm frozen serial sections through the aortic sinus with all three valve leaflets visible as well as the aortic arch with all three branches (left subclavian artery, left common carotid artery, and brachiocephalic artery) visible. For plaque area analysis in aorta, mouse aortas were en face prepared and stained with fresh Oil Red O solution for 2 h at room temperature. Excess of staining was washed out by 70% ethanol. Serial aortic root sections were stained with H&E, oil red O (ORO), or used for immunostaining to detect VSMCs (SM-α-actin, Sigma, F-3777, 1:500), macrophages (anti-Mac2, BD Pharmingen, 553322, 1:900) T cells (anti-CD4, BD Pharmingen, 553043, 1:90; anti-CD8, Chemicon, CBL1318, 1:100), and collagen (0.1% Sirius Red F3BA; Cat# 09400, Polysciences Inc., USA) as previously described.[23] Images were acquired using a Nikon Eclipse TE2000-U microscope. The relative VSMC or macrophage content within the

aortas was quantified by measuring the immunostaining signal positive area using Image-Pro Plus software (Media Cybernetics). CD4+ and CD8+ T cells were counted and quantified as numbers per aortic section. Lesions areas of aorta roots and the thoracic-abdominal aorta were stained for ORO and quantified as described.[19] All the evaluations were carried out by two observers in a blinded manner.

Human Atherosclerotic Specimens

Human normal carotid arteries and atherosclerotic carotid specimens were obtained from the Division of Cardiovascular Medicine at the Brigham and Women's Hospital in accordance with the Institutional Review Board-approved protocol for use of discarded human tissues (protocol #2010-P-001930/2).

Statistical analysis

Prism GraphPad software was used for statistical calculations. Data are represented as mean ± SD unless otherwise stated. Normality of the data was assessed using Shapiro-Wilk test and the equality of group variance was assessed using Brown-Forsythe test. All continuous variables data except Figure VIIK in the online-only Data Supplement passed Shapiro-Wilk and Brown-Forsythe test. Figure VIIK in the online-only Data Supplement was analyzed by rank sum test. Continuous variables were compared using a two-tailed Student's t-test (for comparison between 2 groups) or one-way ANOVA (for comparisons of 3 or more groups) followed by Tukey post hoc pairwise tests. A P value ≤ 0.05 was considered statistically significant.

Results

Identification of smooth muscle cell-specific lncRNA *CARMN* in atherosclerotic lesions.

To identify the presence of lncRNAs in the development of atherosclerosis, RNA was isolated from the aortic intima of $Ldlr^{-/-}$ mice after an athero-progression phase of 0, 2, and 12 weeks on high cholesterol diet (HCD) (groups 1–3) and from a regression phase group (group 4), $Ldlr^{-/-}$ mice fed a HCD for 12 weeks followed by 6 weeks of normal laboratory diet (NLD, Labdiet, 5053, USA) (Figure 1A). Next generation RNA Sequencing (RNA-Seq) was conducted to identify differentially expressed lncRNAs in the development of atherosclerosis. The data was analyzed using DESeq2 and NOR algorithms as previously described.[16] Among the 11 lncRNA transcripts aberrantly expressed in the 4 groups (Figure 1B) was the lncRNA *CARMN*, which decreased in group 3 compared with group 1 during the progression phase (Figure 1B), while increasing in group 4 compared with group 3 during the regression phase (Figure 1C). *CARMN* is a conserved lncRNA expressed in both human and mice. Mouse *CARMN* is a 988 bp, four exon, intergenic transcript (ENSMUST00000182244.7, Figure 1D). A human orthologous transcript (*CARMN*, ENST00000519898.5) was identified by sequence similarity and conserved synteny (53% homology, Figure I in the online-only Data Supplement). Both NCBI and Ensemble databases annotates *CARMN* as a lncRNA and its low coding potential was reported in a previous study.[24]

To determine the expression pattern of *CARMN*, we assessed its expression in the aortic intima and media, lung, heart, liver, skeletal muscle, and peripheral blood mononuclear cells (PBMCs) from C57BL6J mice. *CARMN* was highly expressed in the aortic media and in mouse VSMCs (MOVAS), whereas it was minimally expressed in primary cardiomyocytes, bone-marrow-derived macrophages, or in endothelial cells (bEnd.3) (Figure 1E–F). RNA-ISH demonstrated that *CARMN* localized to the nucleus of MOVAS and human coronary artery smooth muscle cells (HCASMCs) (Figure 1G), which was further validated by RT-qPCR of nuclear and cytoplasmic fractions (Figure 1H). RNA-ISH combined with immunofluorescent staining showed that *CARMN* was enriched in a-SMA positive VSMCs and was not detected in either Mac-2-positive macrophages or CD31-positive endothelial cells in aortic roots from normal or atherosclerotic mice (Figure 1I).

To better understand the regulation of *CARMN* in human atherosclerosis, CARMN expression was assessed in normal human carotid arteries or human atherosclerotic plaques. RNA-ISH combined with immunofluorescent staining showed that CARMN is specific to VSMCs of both normal or atherosclerotic arteries (Figure 1J, Figure II in the online-only Data Supplement). CARMN colocalized with a-SMA in both human and mouse atherosclerosis lesions (Figure 1I, arrow, Figure II in the online-only Data Supplement). RT-qPCR analysis of *CARMN* expression in human VSMCs (HCASMCs), PBMCs, and endothelial cells (human umbilical vein endothelial cells, HUVECs) also showed that *CARMN* is abundantly expressed in VSMCs (Figure 1K). Furthermore, RT-qPCR revealed that *CARMN* expression was decreased in human atherosclerotic plaques compared with non-atherosclerotic arteries (Figure 1L).

CARMN knockdown suppressed VSMC proliferation and atherosclerotic lesion formation.

To further explore the role of *CARMN* in the progression of atherosclerosis, $Ldlr^{-/-}$ mice were intravenously injected with gapmeRs specific to *CARMN* RNA (10 mg/kg, twice weekly, over 12 weeks on HCD compared to negative control gapmeRs (Figure 2A). GapmeR-mediated silencing of *CARMN* effectively reduced its expression in both the aortic intima and media by 44% ($p=0.01$) and 61% ($p<0.001$), respectively(Figure 2B). Furthermore, lesional knockdown of *CARMN* in the aortic intima and media specific to VSMC could be shown by co-staining of a-SMA and CARMN RNA-ISH (Figure 2C). There was no effect of CARMN expression in PBMCs, where basal expression was not detectable, and a modest reduction in very low expression of *CARMN* in the spleen (Figure III in the online-only Data Supplement). The lesion burden in the aortic root and descending aorta was reduced by 29% ($p=0.001$) and 38% ($p=0.004$), respectively, upon silencing of *CARMN* compared to the control group (Figure 2D–E). The necrotic area across the two groups was not affected (Figure 2F).

To determine how cell type composition and extracellular matrix may have contributed to the reduced lesion area in CARMN knockdown $Ldlr^{-/-}$ mice, aortic root sections were stained with markers for VSMC, macrophage, CD4 T cells, CD8 T cells, and for collagen. Lesions with lower CARMN expression had significantly reduced VSMCs and collagen content (Figure 2E and 2H), while no significant change could be observed for macrophages, $CD4^+$ T cells or $CD8^+$ T cells in the lesions (Figure 2G, and 2I–K). To

explore phenotypic differences in lesional VSMCs, proliferation and apoptosis was assessed by co-staining of a-SMA with Ki67, PCNA, or cleaved caspase3. *CARMN* knockdown markedly reduced the number of $Ki67^{+}$a-SMA^{+} cells by 45% (p=0.001, Figure 2M) and the number of $PCNA^{+}$ a-SMA^{+} cells by 43% (p=0.02, Figure XII in the online-only Data Supplement). No significant difference in apoptotic VSMCs between the control and *CARMN* gapmeR treated groups were observed (Figure 2M). In summary, these findings suggest that *CARMN* deficiency alters the proliferative potential of VSMCs without affecting apoptosis in atherosclerotic lesions.

We further assessed for other potential systemic contributors that might impact lesion formation in these mice. There was no significant difference in weight, blood pressure, plasma cholesterol, triglycerides, high-density lipoproteins (HDLs), or low-density lipoproteins (c-LDLs) between control and *CARMN* knockdown groups (Table III in the online-only Data Supplement). Because inflammation is critical for the initiation and progression of atherosclerosis[25], we assessed expression of inflammatory markers in the plasma and aortic intima. *CARMN* knockdown did not alter levels of IL-1β, IL-6, or TNF-α in plasma nor mRNA levels of these cytokines in the aortic intima (Figure IV in the online-only Data Supplement), suggesting that the observed lower plaque burden in *CARMN* knockdown mice is independent of inflammation. Also, plasma alanine transaminase (ALT), aspartate transaminase (AST), and creatinine levels were not significantly altered, excluding adverse effects due to liver toxicity upon gapmeR administration (Table III in the online-only Data Supplement).

CARMN knockdown suppressed VSMC differentiation in *vivo*

To explore the role of CARMN in VSMC differentiation, contractile VSMC markers such as ACTA2, SM22a, MYH11, and CNN1 were detected in the aortic intima and media from control and CARMN knockdown HCD-fed $Ldlr^{-/-}$ mice. RT-qPCR analysis showed that *CARMN* knockdown significantly reduced *ACTA2*, *SM22a*, *MYH11*, *CNN1* expression in both the aortic intima and media (Figure 3A and 3B). In addition, RNA-ISH and immunofluorescent staining revealed that CARMN knockdown reduced *SM22a*, *SM MHC*, *CNN1*, and *a-SMA* expression in the media of the aortic arch (Figure 3C).

CARMN knockdown ameliorated dysregulated cell processes classically involved in atherosclerosis in mice.

We performed a transcriptomic analysis from RNA derived from the aortic intima or media from $Ldlr^{-/-}$ mice injected with control-gapmeR and *CARMN*-gapmeR after 12 weeks. RNA sequencing (RNA-seq) profiling captured 509 differentially expressed genes in the intima and 1,254 differentially expressed gene in the media (false discovery rate (FDR), <0.05) (Figure 4A, and Figures XV–XVII in the online-only Data Supplement). Gene set enrichment analysis on the set of differentially expressed genes (adjusted P-value < 0.05)[26] along with GOcircle and GOchord plots of enriched pathways from both the intima and media datasets showed attenuation of cell adhesion, membrane raft assembly, chemotaxis, cell migration, and inflammatory response following *CARMN* knockdown *in vivo*. (Figure 4B–E). There were 111 genes that were significantly dysregulated in both the intima and media (Figure 4A) and these genes were found to be significantly

involved in inflammatory response, chemotaxis, and membrane associated processes. These data highlight that *CARMN* knockdown impacts pathways likely associated with VSMC proliferation and migration.

CARMN knockdown inhibited VSMC proliferation, migration, and differentiation in *vitro*

We next assessed how *CARMN* knockdown in vitro impacts VSMC function. *CARMN* gapmeR or antisense oligonucleotide (ASO) effectively reduced *CARMN* expression in both MOVAS and HCASMCs in the presence or absence of TGF-β1 treatment, a known stimulant of VSMC proliferation (Figure 5A and 5B, Figure X, Figure XIA and XIB in the online-only Data Supplement). *CARMN* knockdown significantly suppressed both basal and TGF-β1-induced VSMC proliferation (Figure 5C and 5D, Figure XID in the online-only Data Supplement) and migration (Figure 5E and 5F, Figure XIC in the online-only Data Supplement). *CARMN* knockdown significantly reduced expression of VSMC differentiation markers (SM22A, ACTA2, CNN1, MYH11) in both MOVAS and HCASMCs (Figure VA–H in the online-only Data Supplement). Moreover, TGF-β1-induced elevations in protein levels of these markers was reversed by *CARMN* knockdown in MOVAS and HCASMCs (Figure 5G – 5J; and Figure V in the online-only Data Supplement). Immunofluorescent staining also validated that *CARMN* knockdown significantly reduced aortic media levels of SMC markers SM22a, SM MHC, Calponin, and a-SMA in vitro (Figure 5G and 5I). Additionally, *CARMN* knockdown significantly suppressed C-kit expression in the aortic intima and media, and OCT4 and Sca1 expression in HCASMCs in *vitro* (Figure XIE and XIF in the online-only Data Supplement).

CARMN overexpression increased VSMCs proliferation, migration, and differentiation in *vitro*

To explore the effects of *CARMN* overexpression on VSMC function, HCASMCs were transfected with a pcDNA3 vector carrying the full-length sequence of *CARMN*. RT-qPCR analysis showed that *CARMN* expression was significantly increased in HCASMCs transfected with pcDNA3-CARMN compared with pcDNA3 vector (Figure 6A). Additionally, CARMN overexpression is highly enriched in the nuclear fraction compared to the cytoplasm (Figure XIVC in the Online Data Supplement). CARMN overexpression significantly increased VSMC proliferation and migration (Figure 6B and 6C), even at lower overexpression levels of *CARMN* (Figure XIV in the Online Data Supplement). Furthermore, RT-qPCR analysis showed that *CARMN* overexpression markedly increased expression of VSMC markers (SM22A, ACTA2, CNN1, MYH11) (Figure 6D). Western blot and immunofluorescent staining revealed that CARMN overexpression significantly increased the expression of VSMC markers such as SM22a, SM MHC, Calponin, and a-SMA (Figure 6E and 6F).

TGF-β1 induced *CARMN* expression in a Smad2/3-dependent manner

TGF-β1 is a hallmark of many vascular diseases and plays a critical role in VSMC plasticity.[12] RT-qPCR analyses revealed that TGF-β1 treatment induced *CARMN* expression in a time- and dose-dependent manner in both MOVAS and HCASMCs (Figure 7A and 7B). *CARMN* expression, as determined by RNA-ISH, was significantly upregulated in VSMCs by TGF-β1 treatment (Figure 1G). As Smad proteins are key downstream regulators

in TGF-β signaling,[27] we investigated the role of Smad2, Smad3, and Smad4 on *CARMN* expression. The expression of *CARMN* decreased when Smad2 or Smad3 was silenced with siRNA in the presence or absence of TGF-β1 stimulation (Figure 7C–E). In contrast, Smad4 knockdown did not affect *CARMN* expression (Figure 7C–E), suggesting that transcription of *CARMN* is Smad2/3 dependent. To determine whether *CARMN* regulates TGF-β1/Smad signaling, Smad protein expression was detected following TGF-β1 stimulation in CARMN-silenced HCASMCs. We found that CARMN knockdown did not affect TGF-β1-induced Smad2 and Smad3 phosphorylation (Figure 7F and 7G).

Because Smad2 and Smad3 are known transcription factors that regulate the expression of several target genes, the role of potential Smad-binding elements (SBEs) was assessed within the promoter region of CARMN. Using JASPAR, a database of transcription factor binding profiles,[28] three predicted SBEs were identified in the promoter region of CARMN (Figure 7H, Table IV in the online-only Data Supplement) including SBE1: from −1675 to −1671 base pairs (bp); SBE2: from −1411 to −1407 bp; and SBE3: from −1119 to −1115 bp). ChIP-qPCR analysis demonstrated that Smad2 or Smad3 binds to SBE1 and SBE3, but not to SBE2 in the CARMN promoter (Figure 7I). The CARMN promoter region between −1 and −2000 bp was cloned into a pGL3-promoter vector and used a luciferase reporter assay to demonstrate that TGF-β1 stimulation increased CARMN promoter activity, while Smad2 or Smad3 silencing significantly reduced CARMN promoter activity (Figure 7J). Furthermore, a series of pGL3 reporter plasmids were constructed containing SBE1 mutation (Mut1), SBE3 mutation (Mut2), or both SBE1 and SBE3 mutation (Mut3) (Figure 7K). Luciferase reporter assays showed that Mut1 and Mut2 partially reduced TGF-β1 induced CARMN promoter activity, and Mut3 fully abolished luciferase activity (Figure 7L). These data suggest that Smad2 or Smad3 directly binds to the CARMN promoter and upregulates CARMN expression.

CARMN regulated VSMCs plasticity independently of the miR143/145 cluster

Recent studies suggest that lncRNAs can regulate neighboring gene expression in a *cis* manner.[29, 30] Interestingly, the *CARMN* loci is directly upstream of the miR143/145 cluster, which are both derived from same host gene (Figure VI in the online-only Data Supplement). miRNA143/145 are two VSMC-specific miRNAs that have been reported to play a crucial role in VSMCs phenotypic switching.[10] Thus, the relationship between CARMN and miR143/145 cluster was investigated to test whether CARMN regulates VSMC function though *cis*-regulation of the miR143/145 cluster. While *CARMN* knockdown inhibited miR143/145 expression (Figure VIIA and VIIB in the online-only Data Supplement), miR143/145 overexpression could not reverse the downregulation of proliferation and migration as observed upon silencing of CARMN (Figure VIIG, VIIH and VII-I in the online-only Data Supplement). Consistently, miR143/145 overexpression could not recover the differentiated VSMC markers (SM MHC, a-SMA, Calponin, SM22a) as diminished by *CARMN* knockdown (Figure VIIJ in the online-only Data Supplement). Moreover, miR-143/145 expression in the aortic intima or media was not significantly different in CARMN knockdown HCD-fed $Ldlr^{-/-}$ mice compared to gapmeR-controls (Figure VIIK in the online-only Data Supplement). Additionally, CARMN knockdown did not affect expression of KLF4, a downstream target of miR-143 and miR-145, *in*

vitro or *in vivo* (Figure XIII in the online-only Data Supplement). Conversely, miR143 or miR145 silencing had no effect on *CARMN* expression (Figure VIIC–F in the online-only Data Supplement). Taken together, these findings indicate that *CARMN* regulates VSMC plasticity independent of the miR143/145 cluster.

CARMN directly interacts with SRF

As CARMN is located in the nucleus, we explored whether CARMN impacted VSMC function by physically interacting with transcription factors. In vitro RNA pull-down assays with biotinylated CARMN and *lacZ* control showed a distinct 55–70 kDa band (Figure 8A), which was identified as SRF by mass spectrometry (MS) (Figure 8B, Table V, and Figure VIII in the online-only Data Supplement). SRF was one of the most enriched binding proteins and was unique among biotinylated *CARMN* binding proteins compared with biotinylated *lacZ* control. In addition, SRF is known to have gene regulatory function and play a critical role in VSMC plasticity[3]. In *vitro* RNA pulldowns further validated that SRF was only detectable in the eluate of biotin-labeled *CARMN* compared to lacZ control (Figure 8A *bottom*). Furthermore, the binding of *CARMN* to SRF was confirmed *in vivo* after i.v. injection of biotin-labeled *CARMN* and SRF was recovered in aortic protein lysates of biotin-labeled *CARMN* injected mice compared to *LacZ* control mice (Figure 8C). Consistently, RNA-ISH of CARMN combined with SRF immunostaining showed that CARMN and SRF colocalized mainly in the nucleus of HCASMCs (Figure 8D). Next, the direct binding of CARMN and SRF was examined through RNA immunoprecipitation (RIP) studies in HCASMC. RIP showed a 4.8-fold enrichment of *CARMN* by an anti-SRF antibody compared to anti-IgG antibody control (Figure 8E).

To explore the possible CARMN binding region to SRF, we assessed the likelihood of protein-RNA interaction by RNA-Protein Interaction Prediction[31]. This predicted binding of the nucleotides (nt) at 800 to 1197 of CARMN to the RING domain (amino acid residues 1–200) of SRF (Figure 8F). To map the CARMN functional motifs corresponding to SRF binding, we performed an *in vitro* RNA pull-down assay using a series of truncated CARMN fragments. This analysis showed that the CARMN 1–800 nt fragment is sufficient to interact with SRF protein, while the CARMN 1–600 nt fragment could not (Figure 8G). These data suggested that the CARMN 600–800 nt fragment of CARMN may bind with SRF. To investigate if the CARMN 800–1197 nt fragment binds to SRF, we further designed a truncated CARMN 800–1197 nt fragment or deletion mutants of the CARMN 600–800 nt region. Deletion of the CARMN 600–800 nt region or the CARMN 800–1197 nt fragment had reduced binding to SRF, but both did not fully abolish the interaction. (Figure 8H). These data suggested that both CARMN 600–800 nt and 800–1197 nt fragments are necessary for CARMN to bind to the SRF protein.

SRF is required for the regulatory role of *CARMN*

SRF is a transcription factor that regulates VSMC gene expression, thus we further investigated the effect of SRF silencing on CARMN expression. SRF protein expression was effectively diminished by siRNA mediated knockdown (Figure IXC in the online-only Data Supplement) and RT-qPCR analysis showed that SRF silencing did not change *CARMN* expression in HCASMCs (Figure IXD in the online-only Data Supplement). Next, the

effect of *CARMN* knockdown was explored on SRF expression. Interestingly, *CARMN* knockdown had no effect on the expression of SRF *in vitro and vivo* (Figure IXA and IXB in the online-only Data Supplement), which suggests that *CARMN* may regulate the transcriptional activity of SRF at the promoter level of its target genes. ChIP-qPCR validated that *CARMN* knockdown significantly reduced SRF occupancies on the promoters of VSMC targets, including ACTA2, SM22a, MYH11, and CNN1. Furthermore, ChIP-qPCR analysis showed that *CARMN* overexpression significantly increased SRF's occupancies on the promoters of VSMC targets (Figure 9A–D) and c-fos (Figure 9I). Conversely, SRF silencing reversed the upregulation of VSMC markers (SM MHC, a-SMA, Calponin, SM22a) induced by CARMN overexpression (Figure 9G–K). Taken together, these findings indicate that SRF is required for the regulatory role of *CARMN*.

Discussion

VSMC plasticity plays a critical role in the development of a range of vascular occlusive disease states including atherosclerosis.[3, 4] While some studies using different mouse models indicate that inhibition of VSMC proliferation may adversely impact atherosclerotic plaque stability, other studies indicate a stronger impact on lesion formation.[1, 2] In this report, we provide evidence that the VSMC-enriched lncRNA *CARMN* regulates VSMC proliferation by interacting with SRF, a key transcription factor involved in SMC phenotypic switching. In support, lncRNA *CARMN* was dynamically regulated during atherosclerosis progression after 12 weeks of HCD in $Ldlr^{-/-}$ mice, a time point associated with increased VSMC proliferation. Furthermore, silencing of *CARMN* reduced atherosclerosis lesion formation and suppressed VSMCs proliferation, migration, and differentiation in *vivo* and in *vitro (*Figures 2–4). Notably, these effects on lesion formation were independent of differences between groups in the lipoprotein profile, lesional accumulation of leukocytes, or inflammatory markers (Figure IV and Table III in the online-only Data Supplement), indicating that *CARMN* deficiency regulated a distinct process. The expression of *CARMN* was positively regulated by the TGF-β1/Smad2/3 pathway, and *CARMN* overexpression promoted VSMC proliferation, migration, and differentiation (Figure 5). Mechanistically, *CARMN* modulated VSMC plasticity by interacting with SRF and enhancing SRF's occupancy on the promoter regions of its downstream VSMC gene targets.

Accumulating studies highlight that lncRNAs play critical roles in cardiovascular disease and exact their functions through diverse mechanisms.[18, 32] LncRNAs are often expressed in a tissue- and cell-specific manner.[33, 34] By regulating key aspects of cellular function in a cell or tissue-specific manner, lncRNAs provide feasible targets for disease treatment, thereby avoiding or reducing nonspecific or off-target effects. Examples of other cell-specific lncRNAs implicated in atherosclerosis include *SMILR*, a VSMC-enriched lncRNA that promotes cell proliferation by directly regulating mitotic progression.[21] The macrophage-enriched lncRNA *RAPIA* exerts atheroprotective effects by regulating the miRNA-183–5p/ITGB1 pathway[33], whereas the macrophage-specific lncRNA *MAARS* regulates macrophage apoptosis and atherosclerotic lesion formation.[19] Finally, the endothelial-enriched lncRNA *SNHG12* controls DNA damage in the vessel wall, vascular senescence, and atherogenesis.[16] In this study, we validated that *CARMN* is a VSMC-enriched lncRNA in both mouse and human atherosclerotic arteries and VSMC cell lines

using a combination of RNA-ISH, immunofluorescent staining, and RT-qPCR expression analyses (Figure 1).

This study demonstrates how silencing of a lncRNA in atherosclerotic lesions using the nuclease-resistant LNA-modified gapmeRs can provide robust phenotypic modulation. To explore the role of *CARMN* in VSMCs and atherosclerosis, we silenced *CARMN* expression in aortas of $Ldlr^{-/-}$ mice by i.v. delivery of specific gapmeRs to *CARMN*. *CARMN* expression was effectively reduced in both the aortic intima and media and this was further verified to occur in VSMCs by RNA-ISH and a-SMA staining. Interestingly, we observed that the gapmeR delivery not only markedly suppressed *CARMN* expression, but also reduced a-SMA^+ VSMC content in lesions. Functionally, *CARMN* knockdown reduced atherosclerotic lesion formation, VSMC proliferation, and collagen content, but did not change VSMC apoptosis, leukocyte subset accumulation, or lesional necrosis. Moreover, there were no differences in other potential confounders such as the circulating lipid profiles, weights, blood pressure, or inflammatory markers. RNA-seq data of aortic intima showed that CARMN KD changed a few immune/inflammatory genes, such as BTLA, SLAMF6, IDOI. However, both RNA-seq data and RT-qPCR results of aortic intima showed CARMN KD did not alter key inflammatory markers gene of atherosclerosis, such as IL-1β, IL-6, or TNF-α. Additionally, we also evaluated these inflammatory markers in the plasma of mice and found that CARMN knockdown did not alter levels of IL-1β, IL-6, or TNF-α in plasma. Collectively, these findings suggest that loss of VSMCs due to reduced lesional VSMC proliferation and collagen content were the main factors that contributed to the reduced atherosclerotic lesions. Consistent with this premise, *CARMN* knockdown suppressed SMC differentiation markers in the media of aortic arch and in HCASMCs in vitro.

TGF-β1 is critical regulator in VSMC plasticity and atherosclerosis.[13, 14, 35] However, the role of lncRNAs as downstream effectors in VSMCs remains poorly understood. We found that *CARMN* expression was positively regulated by TGF-β1 in a time- and dose-dependent manner. TGF-β1 promoted Smad2/3 association with SBEs in the promoter regions of *CARMN* which was further validated by ChIP-qPCR and luciferase reporter assays. To better understanding the mechanism of *CARMN* in regulating VSMCs phenotypic switching, RNA pulldown studies and mass spectrometry were performed to identify novel *CARMN* associated proteins. We first validated that *CARMN* directly interacted with SRF and facilitated SRF's occupancy on the promoter regions of SMC target genes. A previous study showed that miR143/145 is a downstream target of SRF.[10] While we found that *CARMN* knockdown reduced miR143/145 expression, it remained possible that *CARMN* knockdown inhibited SRF binding to the promoter of miR143/145. However, miR143/145 overexpression did not reverse the regulatory role of *CARMN* in VSMCs, which demonstrated that *CARMN* regulates VSMC plasticity independent of the miR143/145 cluster. Finally, *CARMN* deficiency *in vitro* and *in vivo* had no effect on KLF4 expression, a known target of miR-143 and miR-145.

VSMC phenotypic switching is characterized by reduced expression of contractile proteins, but increased capacity for cell proliferation and migration.[1] However, VSMCs appear to be much more complex and versatile than expected in atherosclerosis. This classical theory is still not adequate to explain the VSMC phenotype in atherosclerotic lesions, which has

been shown to strongly express differentiated VSMC markers and can vary in proliferative capacity.[1, 36, 37] In this study, we demonstrated that *CARMN* knockdown suppressed VSMCs proliferation, migration, and differentiation in *vivo* and in *vitro*. The regulatory role *CARMN* in VSMCs plasticity is partially attributed to the interaction of *CARMN* and SRF. SRF is a widely expressed transcription factor that binds CArG boxes in promoter regions of target genes.[38] In VSMCs, SRF regulates two distinct gene programs, VSMC contractile genes and growth-related immediate early genes, for example, Fos/c-fos. Indeed, there was a ~2-fold enrichment of SRF-binding affinity to the promoter of c-fos in the presence of *CARMN* overexpression (Figure 9I). Additionally, CARMN could regulate stem cell markers expression. CARMN knockdown significantly suppressed C-kit expression in the aortic intima and media, and OCT4 and Sca1 expression in HCASMCs in vitro (Figure XIE–F in the online-only Data Supplement). This is likely one of the main mechanisms by which CARMN overexpression promotes VSMCs proliferation. Myocardin is a coactivator of SRF required for VSMC differentiation.[38, 39] TCF21 has been reported to suppress VSMC differentiation by blocking the myocardin-SRF Pathway.[40] LncRNA *MYOSLID* inhibited VSMCs differentiation by blocking nuclear translocation of Myocardin.[41] Rather than inhibition of myocardin-SRF Pathway, *CARMN* exerted its function by directly interacting with SRF. One possible explanation for the regulatory role of *CARMN* in VSMC plasticity is that *CARMN* may promote SRF to regulate both VSMC contractile genes and growth-related genes. In this study, we found that *CARMN* knockdown suppressed SRF's occupancy on the promoter regions of VSMC genes, whereas *CARMN* overexpression promoted SRF's occupancy on these VSMC target genes. Our data suggested that *CARMN* plays a crucial role in regulating SRF binding to promoter regions of target VSMC genes. Furthermore, silencing of SRF abolished the regulatory role of *CARMN* in VSMC plasticity, which validated the *CARMN*-mediated dependency and interaction with SRF. Mechanistically, we demonstrated that *CARMN* directly interacts with SRF protein through its 600–1197 nt region. While the interacting domain of CARMN with SRF is conserved at ~44% from human to mouse on the nucleotide level, future studies will be needed to further clarify whether smaller domains are responsible for the interaction or how secondary structures may contribute. Collectively, these findings highlight an important role for a TGF-β1-Smad2/3-CARMN-SRF signaling axis in the regulation of VSMC plasticity.

Some limitations of this study should be noted. First, future investigation into the role of *CARMN in vivo* using a *CARMN* conditional knockout mouse line may provide additional insights for its role on VSMC plasticity from a genetic perspective. However, therapeutic inhibition of *CARMN* by gapmeR inhibitors also provides potential translational relevancy using antisense oligonucleotide pharmacology directed at *CARMN*. Second, while *CARMN* is a VSMC-enriched lncRNA in the complex cell content of atherosclerotic lesions, we cannot completely rule out minor contributions from other cell types that may undergo "transdifferentation" into VSMCs. Nonetheless, we validated that *CARMN* knockdown was achieved specifically in VSMCs in both the intima and media of atherosclerotic lesions using RNA-ISH for *CARMN* combined with a-SMA staining in VSMCs. Finally, future studies will be required to further define how *CARMN* regulates SRF's occupancy on the specific downstream VSMC gene targets.

Samir et al[24] first identified and characterized a super enhancer-associated lncRNA that regulated cardiac specification, differentiation and homeostasis, and named this lncRNA as CARMEN, (CAR)diac (M)esoderm (E)nhancer-associated (N)oncoding RNA. Interestingly, during the revision process of this manuscript, Vacante et al[42] showed that loss of *CARMN* activated proliferation and migration of HCASMCs and accelerated atherosclerosis using *CARMN* KO mice. However, there are several differences in approaches in vitro and in vivo that may underlie their observations compared to ours including: (1) use of gapmeRs targeting different domains of *CARMN* in vitro; (2) partial knockdown vs. KO to assess CARMN deficiency in vivo; (3) duration of atherosclerosis (12 weeks (ours) vs 18 weeks (theirs); and levels of cholesterol achieved (~905mg/dL (ours) vs ~680mg/dl (theirs)), among others. Another pre-publication study by Dong et al.[43] showed that transfection of antisense oligonucleotides (ASOs) to *CARMN* increased HCASMCs proliferation. However, assessment of proliferation at later time points (5 days) after transfection compared to earlier time points (2 days) may account for these differences between our findings. Indeed, head-to-head comparison of transfection of ASOs and gapmeRs to *CARMN* in HCASMCs at an earlier time point both demonstrate inhibition of smooth muscle cell markers SM22a and ACTA2; however, our gapmeRs to *CARMN* reduced MYH11 expression under basal and TGF-β1 treatment, whereas the ASOs by Dong et al showed no difference in MYH11 (Figure XIA–B in the online-only Data Supplement). Finally, we tested ASOs and gapmeRs in two related functional assays: HCASMCs ‘scratch’ and BrdU assays and both demonstrated inhibition of proliferation and growth, respectively (Figure XIC–D in the online-only Data Supplement). Taken together, these findings indicate there may be important and nuanced differences that underlie strategies in lncRNA-mediated cellular phenotypes *in vitro* and *in vivo*.

In summary, we have identified the VSMC-enriched lncRNA *CARMN* from atherosclerotic lesions as a homeostatic regulator of VSMC plasticity by interaction with SRF. Deficiency of the lncRNA *CARMN* reduced lesional VSMC proliferation and VSMC content leading to decreased atherosclerosis independent of lipid lowering, lesional leukocyte accumulation, apoptosis, or inflammatory markers. *CARMN* is positively regulated by the TGF-β1/Smad2/3 pathway and interacts with SRF to facilitate SRF occupancy on the promoter regions of target genes. Strategies aimed at suppressing *CARMN* expression or blocking its interaction with SRF may provide a novel translational approach to limit VSMC proliferation applicable to a range of vascular proliferative disease states.

Supplementary Material

Refer to Web version on PubMed Central for supplementary material.

Acknowledgments

The authors would like to thank Ana Lay-Hong and Aniket P. Gad for their assistance with immunofluorescence imaging (Harvard Digestive Disease Center, NIH P30DK034854).

Sources of Funding

This work was supported by the National Institutes of Health (HL115141, HL134849, HL148207, HL148355, HL153356 to M.W.F.), and the American Heart Association (18SFRN33900144 and 20SFRN35200163 to M.W.F., 18POST34030395 to S.H.).

Nonstandard Abbreviations and Acronyms

VSMC	Vascular smooth muscle cell
LncRNA	Long noncoding RNA
CARMN	cardiac mesoderm enhancer-associated non-coding RNA
SRF	serum response factor
KLF4	Krüppel-like factor 4
Ldlr	Low density lipoprotein receptor
MOVAS	Mouse vascular smooth muscle cell line
HCASMC	Human Coronary Artery Smooth Muscle Cell
HUVEC	Human umbilical vein endothelial cells
RT-qPCR	Qualificative Real-Time Polymerase Chain Reaction
RIP	RNA immunoprecipitation
RNA-seq	RNA sequencing
RNA-ISH	RNA-in situ hybridization
ChIP	chromatin immunoprecipitation
MS	mass spectrometry
ALT	alanine transaminase
AST	aspartate transaminase
HCD	high cholesterol diet
NLD	normal laboratory diet
TGF-β	transforming growth factor-beta
α-SMA	alpha smooth muscle Actin

References:

1. Basatemur GL, Jorgensen HF, Clarke MCH, Bennett MR, Mallat Z. Vascular smooth muscle cells in atherosclerosis. Nat Rev Cardiol. 2019;16:727–744.doi:10.1038/s41569-019-0227-9 [PubMed: 31243391]
2. Bennett MR, Sinha S, Owens GK. Vascular smooth muscle cells in atherosclerosis. Circ Res. 2016;118:692–702.doi:10.1161/CIRCRESAHA.115.306361 [PubMed: 26892967]

3. Allahverdian S, Chaabane C, Boukais K, Francis GA, Bochaton-Piallat ML. Smooth muscle cell fate and plasticity in atherosclerosis. Cardiovasc Res. 2018;114:540–550.doi:10.1093/cvr/cvy022 [PubMed: 29385543]
4. Liu M, Gomez D. Smooth muscle cell phenotypic diversity. Arterioscler Thromb Vasc Biol. 2019;39:1715–1723.doi:10.1161/ATVBAHA.119.312131 [PubMed: 31340668]
5. Yuan X, Zhang T, Yao F, Liao Y, Liu F, Ren Z, Han L, Diao L, Li Y, Zhou B, He F, Wang L. Tho complex-dependent posttranscriptional control contributes to vascular smooth muscle cell fate decision. Circ Res. 2018;123:538–549.doi:10.1161/CIRCRESAHA.118.313527 [PubMed: 30026254]
6. Wang Z, Wang DZ, Pipes GC, Olson EN. Myocardin is a master regulator of smooth muscle gene expression. Proc Natl Acad Sci U S A. 2003;100:7129–7134.doi:10.1073/pnas.1232341100 [PubMed: 12756293]
7. Chen J, Kitchen CM, Streb JW, Miano JM. Myocardin: A component of a molecular switch for smooth muscle differentiation. J Mol Cell Cardiol. 2002;34:1345–1356.doi:10.1006/jmcc.2002.2086 [PubMed: 12392995]
8. Cherepanova OA, Gomez D, Shankman LS, et al.Activation of the pluripotency factor oct4 in smooth muscle cells is atheroprotective. Nat Med. 2016;22:657–665.doi:10.1038/nm.4109 [PubMed: 27183216]
9. Feinberg MW, Moore KJ. Microrna regulation of atherosclerosis. Circ Res. 2016;118:703–720.doi:10.1161/CIRCRESAHA.115.306300 [PubMed: 26892968]
10. Cordes KR, Sheehy NT, White MP, Berry EC, Morton SU, Muth AN, Lee TH, Miano JM, Ivey KN, Srivastava D. Mir-145 and mir-143 regulate smooth muscle cell fate and plasticity. Nature. 2009;460:705–710.doi:10.1038/nature08195 [PubMed: 19578358]
11. Cheng Y, Liu X, Yang J, Lin Y, Xu DZ, Lu Q, Deitch EA, Huo Y, Delphin ES, Zhang C. Microrna-145, a novel smooth muscle cell phenotypic marker and modulator, controls vascular neointimal lesion formation. Circ Res. 2009;105:158–166.doi:10.1161/CIRCRESAHA.109.197517 [PubMed: 19542014]
12. Low EL, Baker AH, Bradshaw AC. Tgfbeta, smooth muscle cells and coronary artery disease: A review. Cell Signal. 2019;53:90–101.doi:10.1016/j.cellsig.2018.09.004 [PubMed: 30227237]
13. Frutkin AD, Otsuka G, Stempien-Otero A, Sesti C, Du L, Jaffe M, Dichek HL, Pennington CJ, Edwards DR, Nieves-Cintron M, Minter D, Preusch M, Hu JH, Marie JC, Dichek DA. Tgf-[beta]1 limits plaque growth, stabilizes plaque structure, and prevents aortic dilation in apolipoprotein e-null mice. Arterioscler Thromb Vasc Biol. 2009;29:1251–1257.doi:10.1161/ATVBAHA.109.186593 [PubMed: 19325140]
14. Jaffe M, Sesti C, Washington IM, Du L, Dronadula N, Chin MT, Stolz DB, Davis EC, Dichek DA. Transforming growth factor-beta signaling in myogenic cells regulates vascular morphogenesis, differentiation, and matrix synthesis. Arterioscler Thromb Vasc Biol. 2012;32:e1–11.doi:10.1161/ATVBAHA.111.238410 [PubMed: 21979435]
15. Batista PJ, Chang HY. Long noncoding rnas: Cellular address codes in development and disease. Cell. 2013;152:1298–1307.doi:10.1016/j.cell.2013.02.012 [PubMed: 23498938]
16. Haemmig S, Yang D, Sun X, et al.Long noncoding rna snhg12 integrates a DNA-pk-mediated DNA damage response and vascular senescence. Sci Transl Med. 2020;1210.1126/scitranslmed.aaw1868
17. Hu YW, Guo FX, Xu YJ, et al.Long noncoding rna nexn-as1 mitigates atherosclerosis by regulating the actin-binding protein nexn. J Clin Invest. 2019;129:1115–1128.doi:10.1172/JCI98230 [PubMed: 30589415]
18. Haemmig S, Feinberg MW. Targeting lncrnas in cardiovascular disease: Options and expeditions. Circ Res. 2017;120:620–623.doi:10.1161/CIRCRESAHA.116.310152 [PubMed: 28209793]
19. Simion V, Zhou H, Haemmig S, Pierce JB, Mendes S, Tesmenitsky Y, Perez-Cremades D, Lee JF, Chen AF, Ronda N, Papotti B, Marto JA, Feinberg MW. A macrophage-specific lncrna regulates apoptosis and atherosclerosis by tethering hur in the nucleus. Nat Commun. 2020;11:6135.doi:10.1038/s41467-020-19664-2 [PubMed: 33262333]
20. Hung J, Scanlon JP, Mahmoud AD, Rodor J, Ballantyne M, Fontaine MAC, Temmerman L, Kaczynski J, Connor KL, Bhushan R, Biessen EAL, Newby DE, Sluimer JC, Baker AH.

Novel plaque enriched long noncoding rna in atherosclerotic macrophage regulation (pelaton). Arterioscler Thromb Vasc Biol. 2020;40:697–713.doi:10.1161/ATVBAHA.119.313430 [PubMed: 31826651]

21. Mahmoud AD, Ballantyne MD, Miscianinov V, et al.The human-specific and smooth muscle cell-enriched lncrna smilr promotes proliferation by regulating mitotic cenpf mrna and drives cell-cycle progression which can be targeted to limit vascular remodeling. Circ Res. 2019;125:535–551.doi:10.1161/CIRCRESAHA.119.314876 [PubMed: 31339449]
22. Daugherty A, Tall AR, Daemen M, Falk E, Fisher EA, Garcia-Cardena G, Lusis AJ, Owens AP 3rd, Rosenfeld ME, Virmani R, American Heart Association Council on Arteriosclerosis T, Vascular B, Council on Basic Cardiovascular S. Recommendation on design, execution, and reporting of animal atherosclerosis studies: A scientific statement from the american heart association. Arterioscler Thromb Vasc Biol. 2017;37:e131–e157.doi:10.1161/ATV.0000000000000062 [PubMed: 28729366]
23. Sun X, Icli B, Wara AK, Belkin N, He S, Kobzik L, Hunninghake GM, Vera MP, Registry M, Blackwell TS, Baron RM, Feinberg MW. Microrna-181b regulates nf-kappab-mediated vascular inflammation. J Clin Invest. 2012;122:1973–1990.doi:10.1172/JCI61495 [PubMed: 22622040]
24. Ounzain S, Micheletti R, Arnan C, et al.Carmen, a human super enhancer-associated long noncoding rna controlling cardiac specification, differentiation and homeostasis. J Mol Cell Cardiol. 2015;89:98–112.doi:10.1016/j.yjmcc.2015.09.016 [PubMed: 26423156]
25. Libby P, Ridker PM, Hansson GK. Progress and challenges in translating the biology of atherosclerosis. Nature. 2011;473:317–325.doi:10.1038/nature10146 [PubMed: 21593864]
26. Walter W, Sanchez-Cabo F, Ricote M. Goplot: An r package for visually combining expression data with functional analysis. Bioinformatics. 2015;31:2912–2914.doi:10.1093/bioinformatics/btv300 [PubMed: 25964631]
27. Derynck R, Budi EH. Specificity, versatility, and control of tgf-beta family signaling. Sci Signal. 2019;12:eaav5183.doi:10.1126/scisignal.aav5183 [PubMed: 30808818]
28. Khan A, Fornes O, Stigliani A, et al.Jaspar 2018: Update of the open-access database of transcription factor binding profiles and its web framework. Nucleic Acids Res. 2018;46:D1284.doi:10.1093/nar/gkx1188 [PubMed: 29161433]
29. Kopp F, Mendell JT. Functional classification and experimental dissection of long noncoding rnas. Cell. 2018;172:393–407.doi:10.1016/j.cell.2018.01.011 [PubMed: 29373828]
30. Simion V, Zhou H, Pierce JB, Yang D, Haemmig S, Tesmenitsky Y, Sukhova G, Stone PH, Libby P, Feinberg MW. Lncrna vinas regulates atherosclerosis by modulating nf-kappab and mapk signaling. JCI Insight. 2020;510.1172/jci.insight.140627
31. Muppirala UK, Honavar VG, Dobbs D. Predicting rna-protein interactions using only sequence information. BMC Bioinformatics. 2011;12:489–499.doi:10.1186/1471-2105-12-489 [PubMed: 22192482]
32. Jae N, Dimmeler S. Noncoding rnas in vascular diseases. Circ Res. 2020;126:1127–1145.doi:10.1161/CIRCRESAHA.119.315938 [PubMed: 32324505]
33. Sun C, Fu Y, Gu X, et al.Macrophage-enriched lncrna rapia: A novel therapeutic target for atherosclerosis. Arterioscler Thromb Vasc Biol. 2020:1464–1478.doi:10.1161/ATVBAHA.119.313749 [PubMed: 32268789]
34. Ponnusamy M, Liu F, Zhang YH, et al.Long noncoding rna cpr (cardiomyocyte proliferation regulator) regulates cardiomyocyte proliferation and cardiac repair. Circulation. 2019;139:2668–2684.doi:10.1161/CIRCULATIONAHA.118.035832 [PubMed: 30832495]
35. Goumans MJ, Ten Dijke P. Tgf-beta signaling in control of cardiovascular function. Cold Spring Harb Perspect Biol. 2018;1010.1101/cshperspect.a022210
36. Chappell J, Harman JL, Narasimhan VM, Yu H, Foote K, Simons BD, Bennett MR, Jorgensen HF. Extensive proliferation of a subset of differentiated, yet plastic, medial vascular smooth muscle cells contributes to neointimal formation in mouse injury and atherosclerosis models. Circ Res. 2016;119:1313–1323.doi:10.1161/CIRCRESAHA.116.309799 [PubMed: 27682618]
37. Misra A, Feng Z, Chandran RR, Kabir I, Rotllan N, Aryal B, Sheikh AQ, Ding L, Qin L, Fernandez-Hernando C, Tellides G, Greif DM. Integrin beta3 regulates clonality and fate

of smooth muscle-derived atherosclerotic plaque cells. Nat Commun. 2018;9:2073.doi:10.1038/s41467-018-04447-7 [PubMed: 29802249]

38. McDonald OG, Wamhoff BR, Hoofnagle MH, Owens GK. Control of srf binding to carg box chromatin regulates smooth muscle gene expression in vivo. J Clin Invest. 2006;116:36–48.doi:10.1172/JCI26505 [PubMed: 16395403]
39. Onuh JO, Qiu H. Serum response factor-cofactor interactions and their implications in disease. FEBS J. 202010.1111/febs.15544
40. Nagao M, Lyu Q, Zhao Q, Wirka RC, Bagga J, Nguyen T, Cheng P, Kim JB, Pjanic M, Miano JM, Quertermous T. Coronary disease-associated gene tcf21 inhibits smooth muscle cell differentiation by blocking the myocardin-serum response factor pathway. Circ Res. 2020;126:517–529.doi:10.1161/CIRCRESAHA.119.315968 [PubMed: 31815603]
41. Zhao JJ, Zhang W, Lin MY, Wu W, Jiang PT, Tou E, Xue M, Richards A, Jourd'heuil D, Asif A, Zheng DY, Singer HA, Miano JM, Long XC. Myoslid is a novel serum response factor-dependent long noncoding rna that amplifies the vascular smooth muscle differentiation program. Arterioscl Throm Vas. 2016;36:2088–2099.doi:10.1161/Atvbaha.116.307879
42. Vacante F, Rodor J, Lalwani MK, et al.Carmn loss regulates smooth muscle cells and accelerates atherosclerosis in mice. Circ Res. 202110.1161/CIRCRESAHA.120.318688

Highlights

- CARMN is an abundant, VSMC-enriched nuclear lncRNA.
- TGF-β1 regulates CARMN expression in a Smad2/3-dependent manner.
- CARMN regulates VSMC plasticity and atherosclerosis through its interaction with SRF (serum response factor), enhancing its binding to target gene promoters.
- Silencing CARMN reduced atherosclerosis lesion formation and suppressed VSMCs proliferation in atherosclerotic plaques, providing a new therapeutic target for atherosclerosis beyond lipid lowering or anti-inflammatory interventions

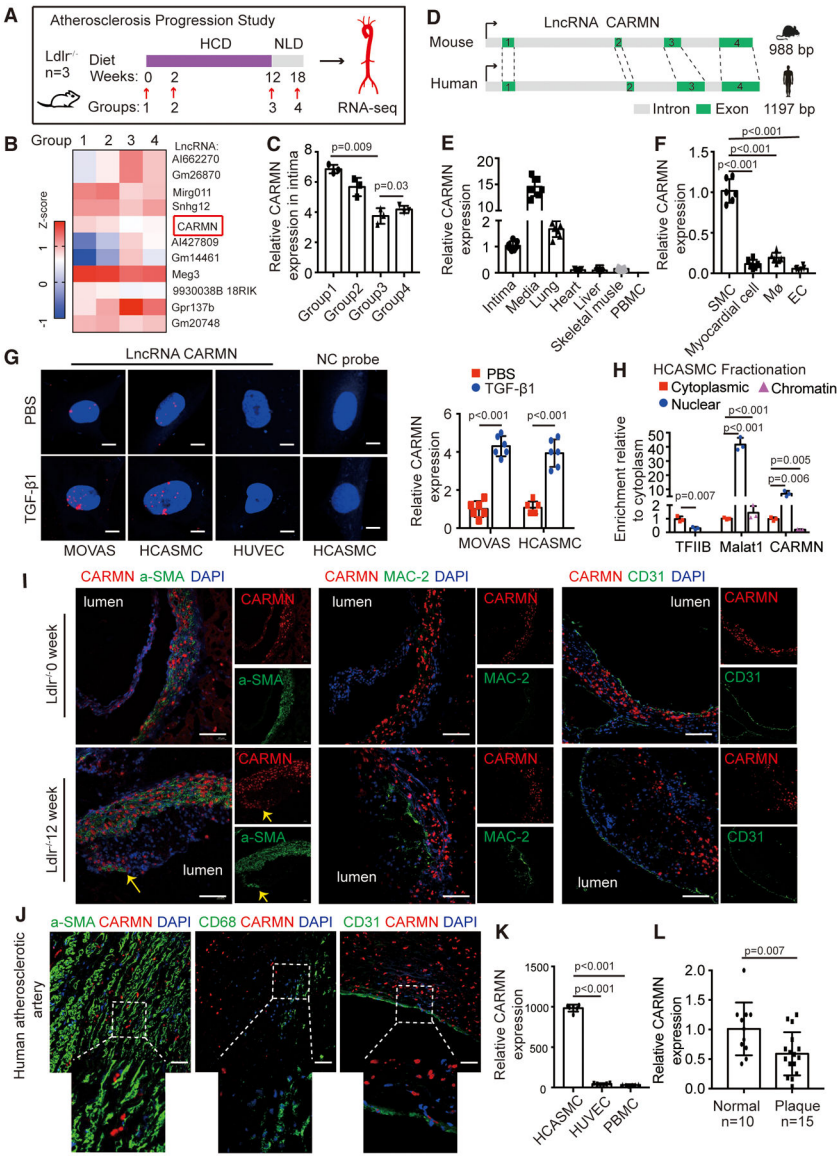

Figure 1. *CARMN* is a vascular smooth muscle cell-enriched lncRNA.

A, RNA derived from aortic intima of Ldlr$^{-/-}$ mice (n = 3) fed with HCD for 0 weeks (group 1), 2 weeks (group 2), 12 weeks (group 3), or 18 weeks (group 4) after 6 weeks of NLD. **B**, LncRNA candidates identified with progression and regression of atherosclerosis in the aortic intima of Ldlr$^{-/-}$ mice. RNA-seq data are available through the Gene Expression Omnibus (GSE138219). **C**, RNA-Seq results for CARMN across groups 1–4 obtained by RNA-seq analysis. **D**, Schematic representation of mouse and human CARMN transcripts and RNA size. **E**, RT-qPCR analysis of CARMN expression in different organs or tissues isolated from C57BL/6J mice (n=6). **F**, RT-qPCR analysis of CARMN expression in VSMCs (MOVAS), primary myocardial cells, macrophages (bone marrow-derived macrophages), and endothelial cells (bEnd.3) (n=6). **G**, Representative confocal FISH images showing nuclear localization of CARMN (red dots) in MOVAS, human coronary artery smooth muscle cells (CASMC), and human umbilical vein endothelial

cells (HUVEC). Quantification of CARMN expression in MOVAS and HCASMC after the treatment of TGF-β1 for 24 h (n=6). Scale bar = 10 μm. **H**, RT-qPCR analysis for RNA derived HCASMC separated into cytoplasmic, nuclear, and chromatin fractions and normalized to the cytoplasmic fraction (n=3). **I**, RNA-ISH for CARMN and a-SMA, Mac-2, or CD31 staining in the regions of the aorta root with and without atherosclerotic lesions of $Ldlr^{-/-}$ mice. Arrow represents the colocalization of CARMN and a-SMA in atherosclerotic lesions. Scale bar = 200 μm. **J**, Representative image of CARMN (red dots) colocalization with $a\text{-}SMA^{+}$ VSMCs, $CD68^{+}$ macrophages, and $CD31^{+}$ endothelial cells in human atherosclerotic arteries. Scale bar = 200 μm. **K**, RT-qPCR analysis of CARMN expression in the indicated human cells (n=6). **L**, RT-qPCR analysis of CARMN expression in human normal carotid artery (n=10) and atherosclerotic plaques (n=15). Data are expressed as the means ± SDs. P value was determined by student t-test or one-way ANOVA with Fisher's test.

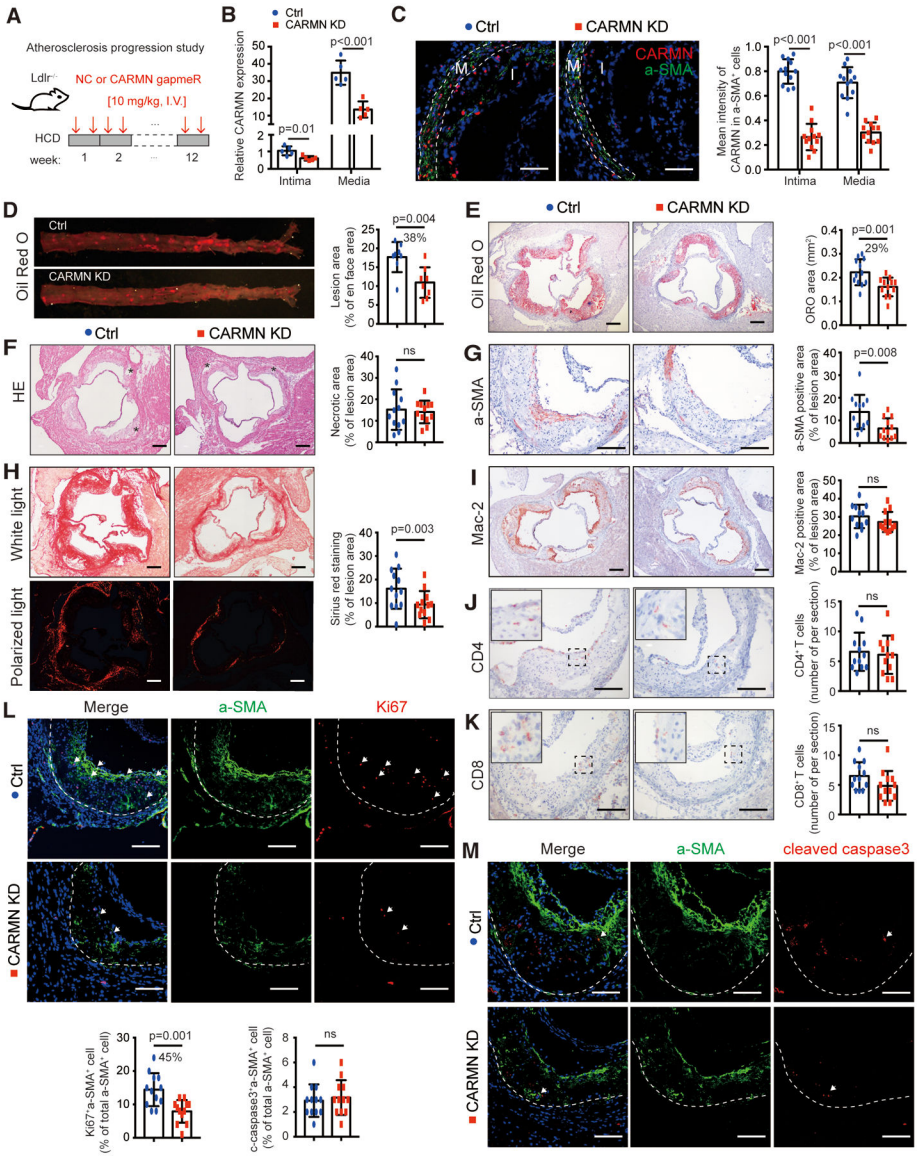

Figure 2. *CARMN* knockdown suppressed atherosclerotic lesion formation and VSMC proliferation in vivo.

A, *Ldlr*$^{-/-}$ mice were intravenously injected with control gapmeR or CARMN gapmeR (n=15, 10mg/kg/mouse) twice per week and continuously fed with high cholesterol diet (HCD) for 12 weeks. **B**, RT-qPCR analysis of CARMN expression in aortic intima and media. **C**, RNA-ISH for CARMN (red) and a-SMA (green) staining in aortic root and quantification of mean intensity of CARMN in a-SMA$^+$ cells in aortic media and intima (n=12). M, media; I, Intima. Scale bar: 50 μm. **D** and **E**, Representative image and quantification of Oil Red O staining in descending aorta (**D**, n=8) and aortic root (**E**, n=12). Scale bar: 100 μm. **F-K**, In the aortic root, lesions were assessed by (**F**) H&E (necrosis), (**G**) a-SMA$^+$ (VSMCs), (**H**) Picrosirius red (collagen), (**I**) Mac-2$^+$ (macrophages), (**J**) CD4$^+$ (T cells), (**K**) CD8$^+$ (T cells). * represents necrotic area. Scale bar: 100 μm. n=12 per group. **L**, Representative image of Ki67 (red), a-SMA (green) staining in aortic root and quantification of Ki67$^+$a-SMA$^+$ cells in total a-SMA$^+$ cells (n=12). Scale bar: 100 μm. M, Representative

image of Cleaved-Caspase3 (red), a-SMA (green) staining in aortic root and quantification Cleaved-Caspase3^{+}a-SMA^{+} cells in total a-SMA^{+} cells (n=12). Scale bar: 100 μm. Data are expressed as the means ± SDs. P value was determined by student t-test. ns=no significant.

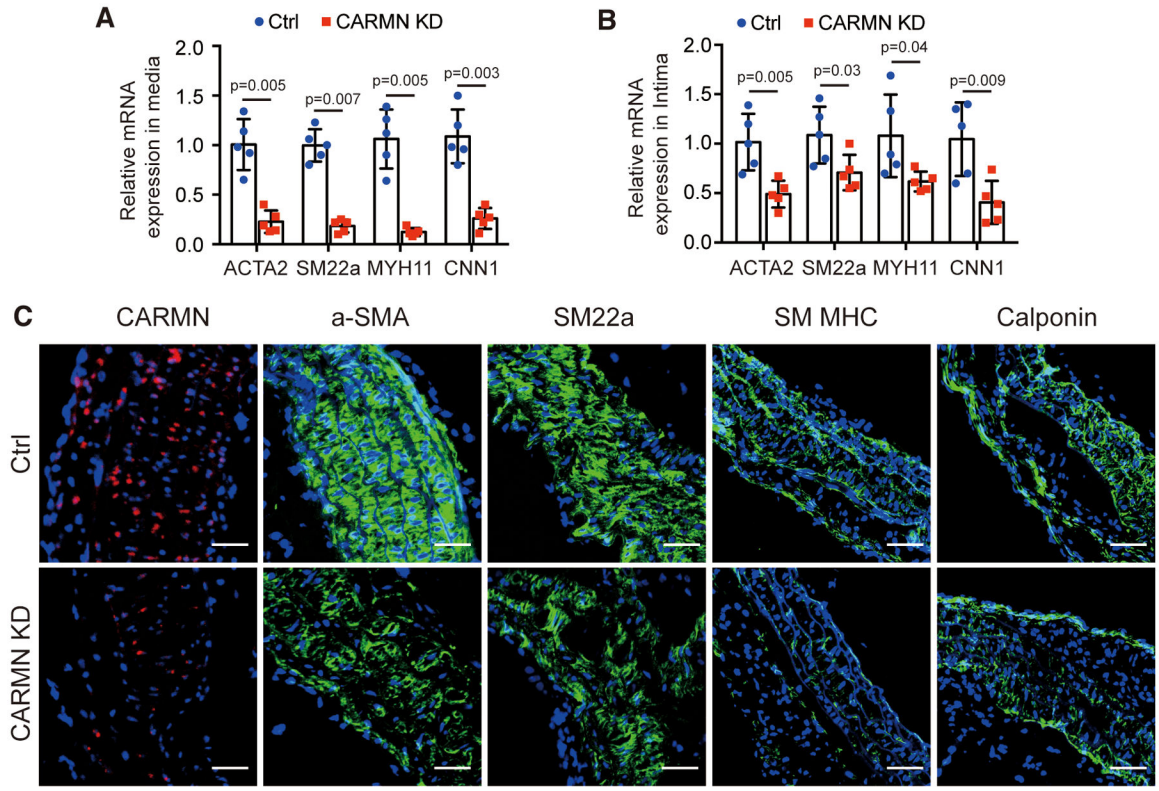

Figure 3. CARMN knockdown suppressed vascular smooth muscle cell (VSMC) marker gene expression in vivo.

A and **B**, RT-qPCR analysis of VSMC markers (ACTA2, SM22a, MYH11, CNN1) expression in aortic media (A) or intima (B) from control and CARMN knockdown $Ldlr^{-/-}$ mice (n=5). **C**, RNA-ISH of CARMN and immunofluorescent staining of VMSC markers in media of aortic arch from control and CARMN knockdown $Ldlr^{-/-}$ mice. Scale bar: 100 μm. Data are expressed as the means ± SDs. P value was determined by student t-test.

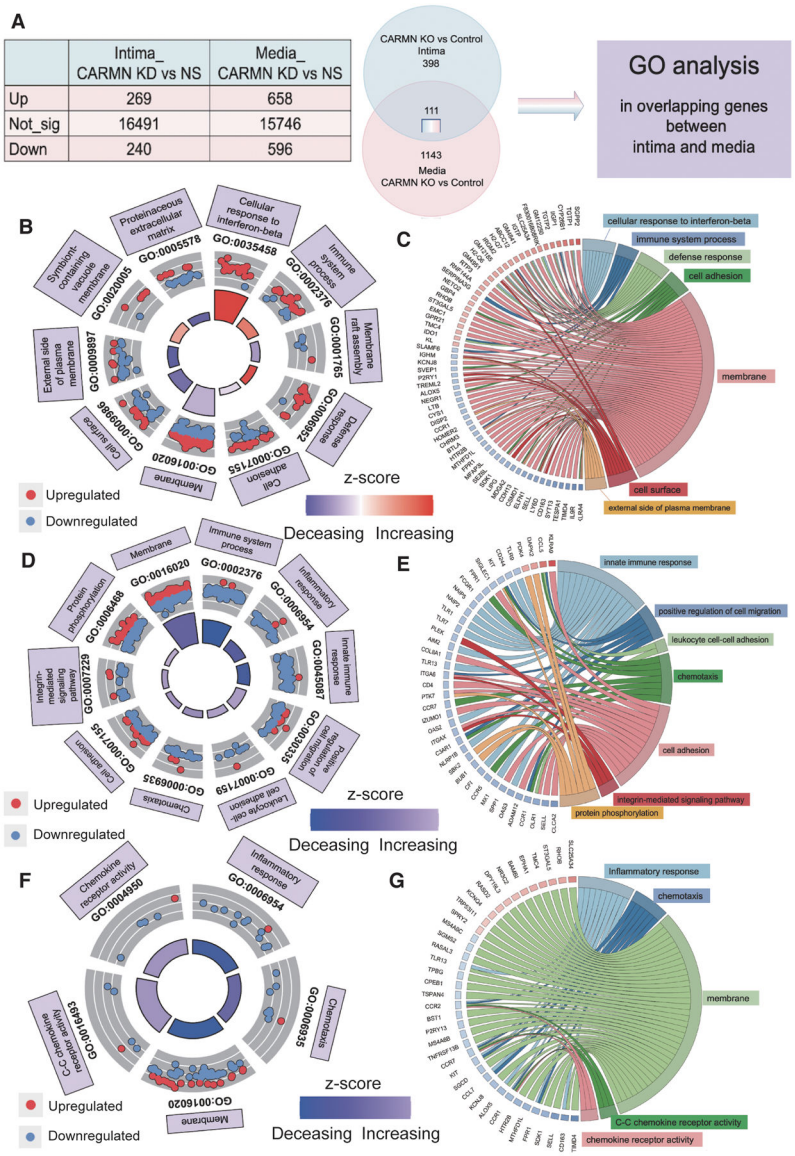

Figure 4. Genome-wide RNA-seq analysis of aortic intima and media from Ldlr$^{-/-}$ mice injected with control gapmeR or CARMN gapmeR.

A, Differentially expressed genes in aortic intima and media in control-gapmeR and CARMN-gapmeR treated *Ldlr*$^{-/-}$ mice (FDR, <0.05). **B**, GOCircle plot of significantly dysregulated mRNA pathways (Bonferroni, <0.05) in aortic intima from control-gapmeR versus CARMN-gapmeR treated mice. The inner ring contains a bar plot where the height of the bar indicates the significance of the term (−log10 adjusted P-value), and color corresponds to the z-score. The outer ring displays dot plots of the expression levels (logFC) for the genes in each term. **C**, GOChord plot showing the significantly regulated genes (log2 fold change, >1.5; FDR, <0.05) involved in the top 7 enriched pathways in the aortic intima from control-gapmeR versus CARMN-gapmeR treated mice. The genes were linked via ribbons to the assigned GO terms and blue-to-red coding next to the selected genes indicated log-fold change of the genes. **D**, GOCircle plot of significantly dysregulated mRNA pathways (Bonferroni, <0.05) in the aortic media from control-gapmeR versus

CARMN-gapmeR treated mice. **E,** GOChord plot showing the significantly regulated genes (log2 fold change, >1.5; FDR, <0.05) involved in the top 7 enriched pathways in aortic media. **F,** Gene set enrichment analysis on the 111 significantly differentially expressed genes overlapping between intima and media transcriptome analyses. **G,** GOChord plot showing the significantly regulated genes (FDR, <0.05) involved in the enriched pathways (Bonferroni, <0.05) in the overlapping gene set between intima and media.

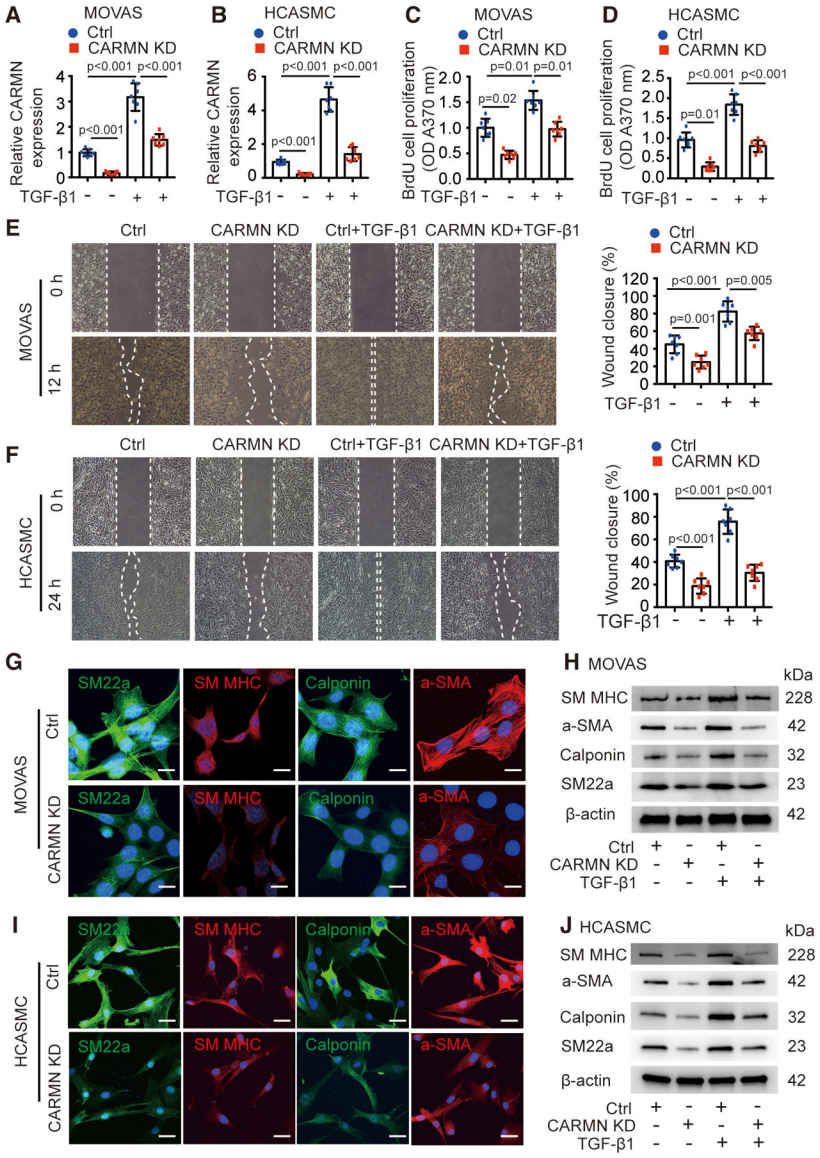

Figure 5. *CARMN* knockdown inhibited VSMC proliferation, migration, and differentiation in *vitro*.

A, RT-qPCR analysis of CARMN expression in gapmeR transfected MOVAS with or without TGF-β1 (5 ng/mL) stimulation. **B**, RT-qPCR analysis of CARMN expression in gapmeR transfected CASMC with or without TGF-β1 (1 ng/mL) stimulation. **C**, BrdU cell proliferation assay and quantitative analysis were performed to detect cell proliferation in gapmeR transfected MOVAS with or without TGF-β1 (5 ng/mL) stimulation (n=6). **D**, BrdU cell proliferation assay and quantitative analysis were performed to detect cell proliferation in gapmeR transfected CASMC with or without TGF-β (1 ng/mL) stimulation (n=6). **E**, Cell migration assay and quantitative analysis were performed to detect cell migration in gapmeR transfected MOVAS with or without TGF-β1 (5 ng/mL) stimulation (n=6). **F**, Cell migration assay was performed to detect cell migration in gapmeR transfected MOVAS with or without TGF-β1 (5 ng/mL) stimulation (n=6). **G**, Immunofluorescent staining of SM22a, SM MHC, Calponin, and a-SMA in gapmeR transfected MOVAS. Scale bar = 20

μm. **H**, Western blot was performed to detect the SM22a, SM MHC, Calponin, and a-SMA expression in gapmeR transfected MOVAS with or without TGF-β1 (5 ng/mL) stimulation (n=4). Scale bar = 20 μm. **I**, Immunofluorescent staining of SM22a, SM MHC, Calponin, and a-SMA in gapmeR transfected HCASMC. Scale bar = 20 μm. **J**, Western blot was performed to detect the SM22a, SM MHC, Calponin, and a-SMA expression in gapmeR transfected HCASMC with or without TGF-β1 (1 ng/mL) stimulation (n=4). Data are expressed as the means ± SDs. P value was determined by one-way ANOVA with Fisher's test.

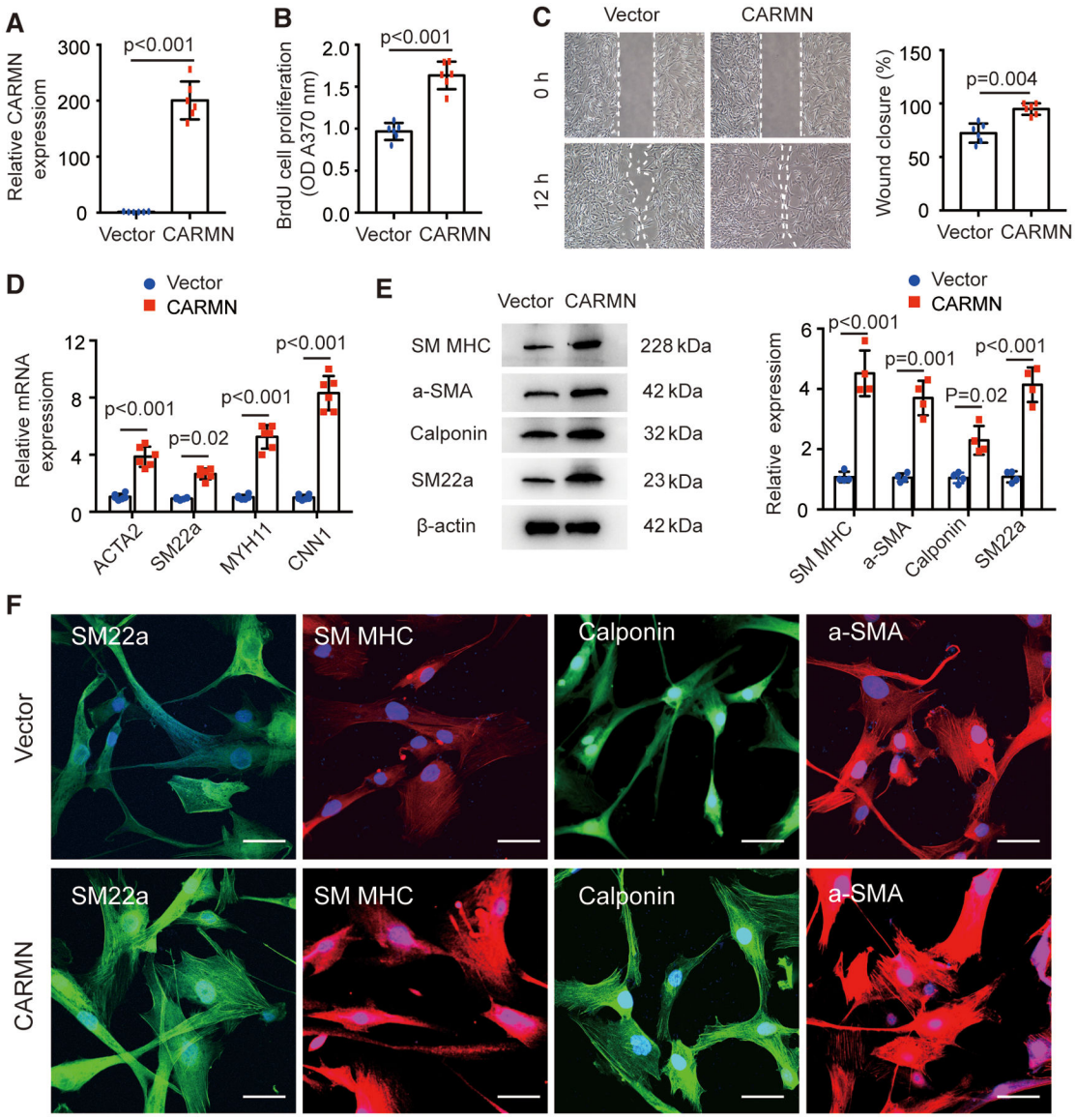

Figure 6. *CARMN* overexpression increased VSMCs proliferation, migration, and differentiation in *vitro*.

A, RT-qPCR analysis of CARMN expression in pcDNA3 vector or pcDNA3-CARMN transfected HCASMC (n=6). **B**, BrdU cell proliferation assay and quantitative analysis were performed to detect cell proliferation in pcDNA3 vector or pcDNA3-CARMN transfected HCASMC (n=6). **C**, Cell migration assay and quantitative analysis were performed to detect cell migration in pcDNA3 vector or pcDNA3-CARMN transfected HCASMC (n=6). **D**, RT-qPCR analysis of *SM22a*, *SM MHC*, *Calponin*, and *a-SMA* mRNA expression in pcDNA3 vector or pcDNA3-CARMN transfected HCASMC (n=6). **E**, Western blot and quantification were performed to detect the SM22a, SM MHC, Calponin, and a-SMA expression in pcDNA3 vector or pcDNA3-CARMN transfected HCASMC (n=4). **F**, Immunofluorescent staining of SM22a, SM MHC, Calponin, and a-SMA in pcDNA3 vector or pcDNA3-CARMN transfected HCASMC. Scale bar = 20 μm. Data are expressed as the means ± SDs. P value was determined by student t-test.

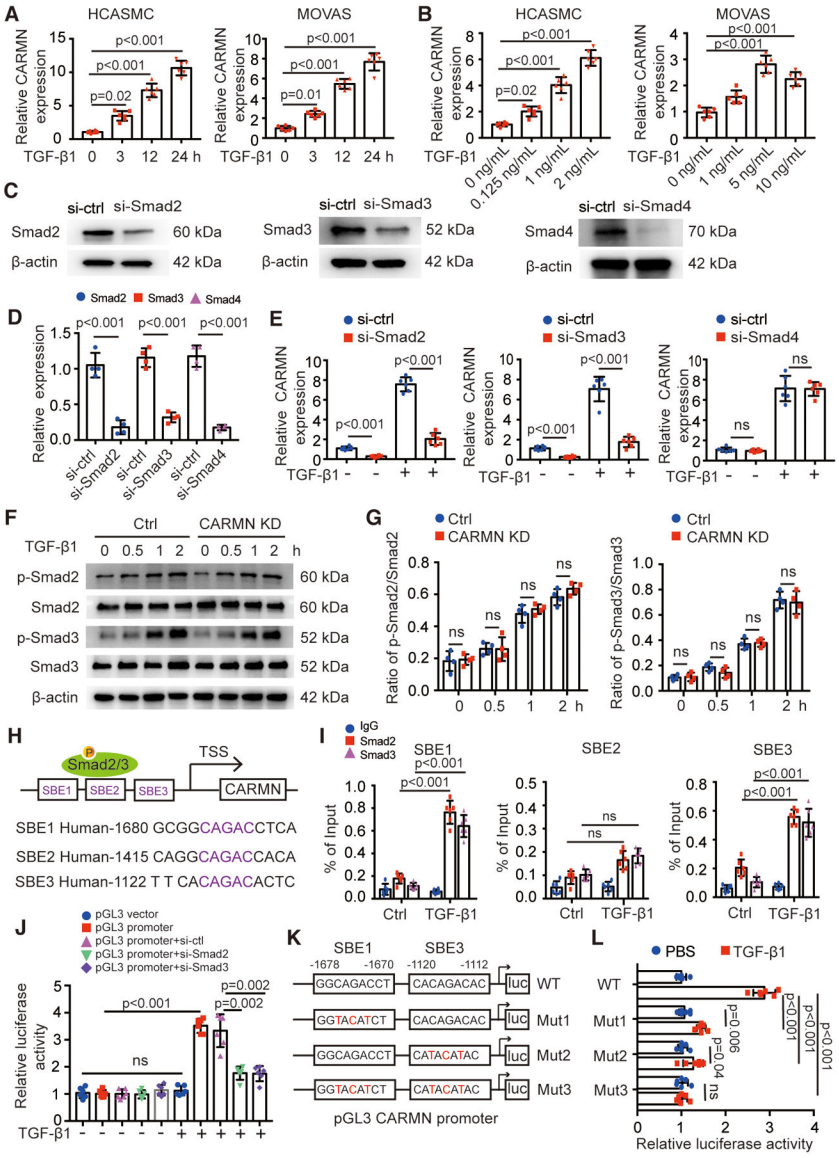

Figure 7. TGF-β1 induced *CARMN* expression in a Smad2/3 dependent manner.

A, RT-qPCR analysis of CARMN expression in HCASMC or MOVAS treated with hTGF-β1 (2 ng/mL) or mTGF-β1 (10 ng/mL) for indicated times (n=6). **B**, RT-qPCR analysis of CARMN expression in HCASMC or MOVAS treated with indicated concentration of hTGF-β1 or mTGF-β1 for 24 h (n=6). **C** and **D**, Western blot and quantitative analysis of Smad2, Smad3, and Smad4 expression in HCASMC transfected with siRNA of control, Smad2, Smad3, and Smad4 for 48 h, respectively (n=4). **E**, HCASMCs were transfected with siRNA of control, Smad2, Smad3, and Smad4 for 24 h, and then treated with hTGF-β1 (2 ng/mL) for another 24 h and CARMN expression was quantified by RT-qPCR (n=6). **F** and **G**, Western blot and quantitative analysis of Smad2, p-Smad2, Smad3, p-Smad3 expression in control or CARMN gapmeR transfected HCASMC treated with hTGF-β1 (2 ng/mL) for the indicated time(n=4). **H**, Smad binding elements (SBEs) in the region of the CARMN promoter. **I**, ChIP-qPCR assay showing amplification of the Smad binding elements (SBE1,

SBE2, and SBE3) in CARMN promoter using an antibody against Smad2 or Smad3 (n=6). **J**, Relative luciferase activity of CARMN promoter in HCASMC transfected with siRNA of control, Smad2 or Smad3 and treated ± hTGF-β1 (n=6). **K**, Mutation of SBE in the CARMN promoter. **L**, Relative luciferase activity of wild-type (WT) promoter constructs and SBE-site mutants in HCASMC treated ± hTGF-β1 (n=6). Data are expressed as the means ± SDs. P value was determined by student t-test or one-way ANOVA with Fisher's test. ns=no significant.

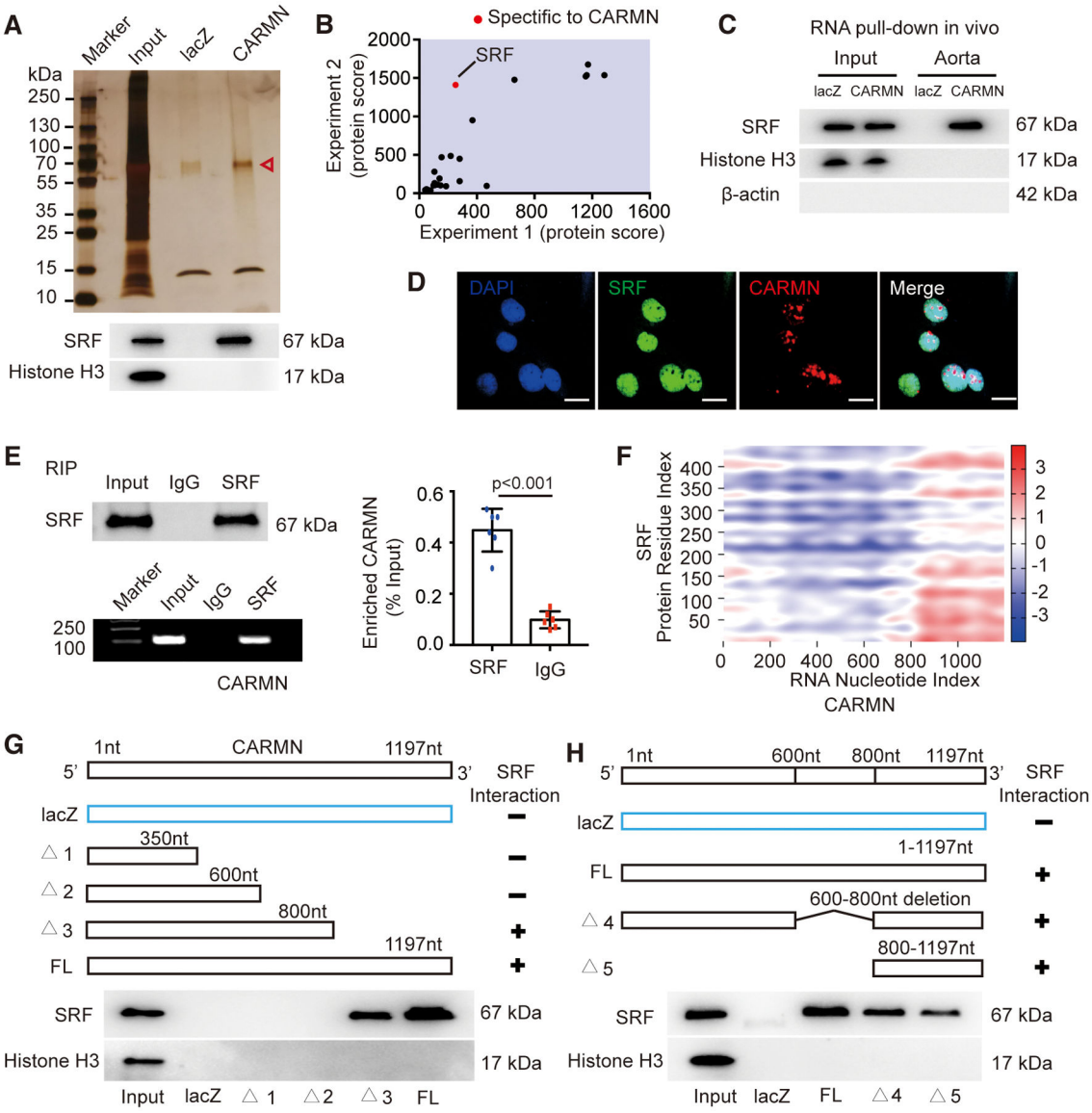

Figure 8. Direct interaction of *CARMN* with serum response factor (SRF).

A, Gel image of silver staining showing proteins pulled down by biotinylated lacZ and CARMN RNA from HCASMC nuclear lysates. Bottom, SRF and Histone H3 protein were detected by Western blotting. **B**, Proteins identified by pulldowns of biotinylated CARMN from two independent biological experiments, two technical replicates each. **C**, In vivo lncRNA pulldown of nuclear protein lysate derived from the aorta of C57BL/6J mice after two intravenous injections of biotin-labeled CARMN or lacZ (n = 4 per group, pooled). **D**, RNA ISH combined with immunofluorescence staining showed colocalization of CARMN and SRF in HCASMC treated with TGF-β1 for 12 h. Scale bar = 10 μm. **E**, Immunoprecipitation of SRF after RNA isolation and subsequent RT-qPCR for CARMN (n = 6). **F**, Predicted interaction of CARMN (nucleotide positions [nt] 800–1198) and SRF protein (amino acid residues 1–200). Red area represents binding signal. **G**, Mapping the SRF interaction region of CARMN. Biotinylated RNAs corresponding to different fragments

of CARMN or lacZ were co-incubated with HCASMC nuclear lysates, and associated SRF proteins were detected by Western blotting. **H**, Serial deletions of CARMN were used in RNA pull-down assays to identify regions required for CARMN and SRF interaction. FL: full length. Data are expressed as the means ± SDs. P value as determined by student t-test.

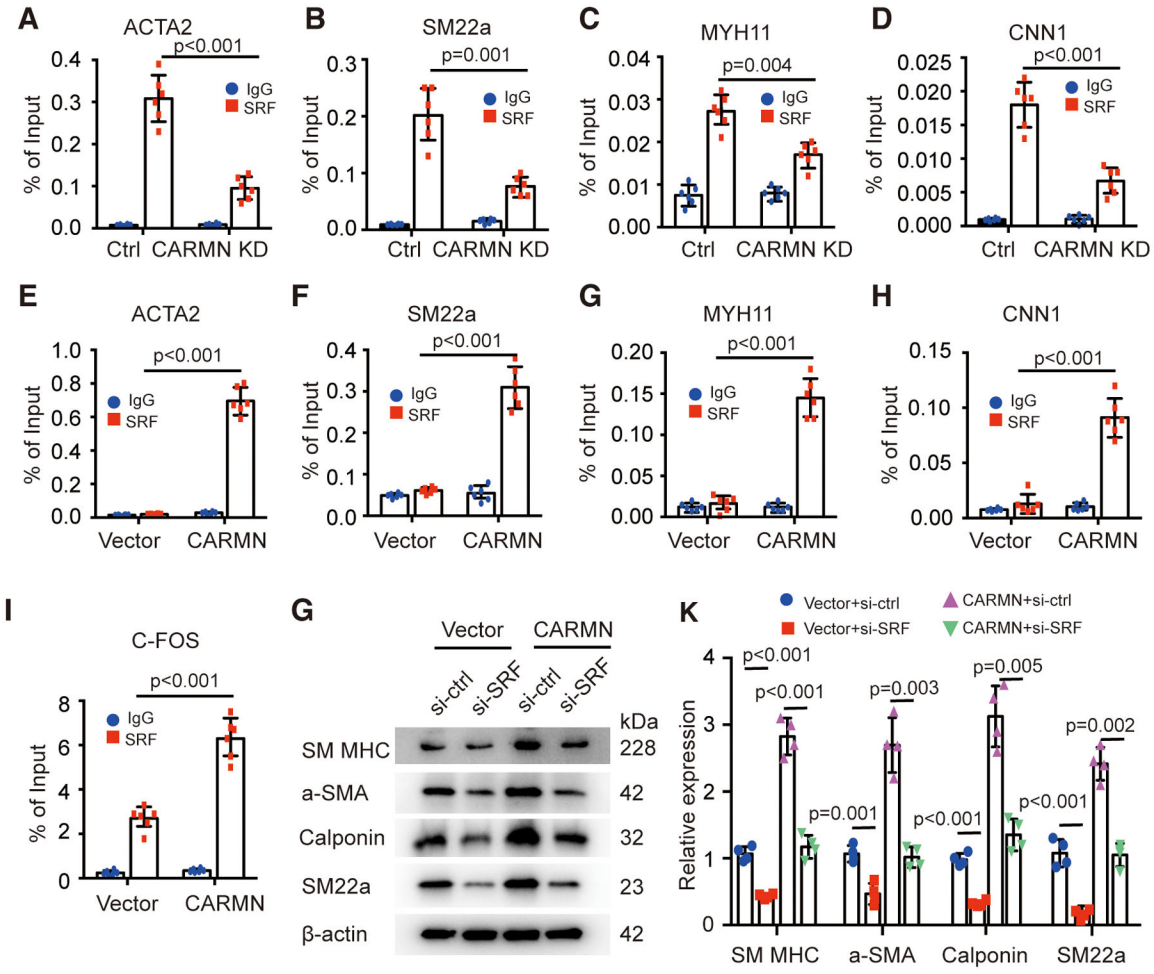

Figure 9. SRF is required for the regulatory role of *CARMN* in VSMCs.

A-D, ChIP-qPCR analysis of SRF occupancy on the promoters of target genes in HCASMC transfected with control or CARMN gapmeR (n=6). **E-I**, ChIP-qPCR analysis of SRF occupancy on the promoters of target genes in HCASMC with stable overexpression of CARMN and empty vector (n=6). **G** and **K**, Western blot and quantification of SRF targets after treatment with SRF siRNAs in HCASMC with stable overexpression of CARMN and empty vector (n=4). Data are expressed as the means ± SDs. P value was determined by one-way ANOVA with Fisher's test.